Big Data and Information Analytics

https://www.aimspress.com/journal/BDIA

BDIA, 10: 374–390.
DOI:10.3934/bdia.2026019
Received: 26 October 2026
Accepted: 31 October 2026
Published: 11 November 2026

Research article

Moment equilibrium and dynamical transitions in a stochastic logistic model: a financial application

Yunihan Wang[1] **and Haiyan Wang**[2,*]

[1] School of Mathematical and Statistical Sciences, Arizona State University, Tempe, AZ 85287–1804, USA

[2] School of Mathematical and Natural Sciences, Arizona State University, Phoenix, AZ 85069, USA

* **Correspondence:** Email: haiyan.wang@asu.edu

Abstract: We study moment-equilibrium transitions in a stochastic logistic difference equation and apply the results to financial credit adjustment. Assuming four lognormal-form input moments, preservation of the mean and variance yields two explicit growth branches and an exact admissibility bound linking input dispersion with multiplicative noise variability. Both real nondegenerate branches lie below the deterministic first period-doubling boundary. An exact variance correction also connects the stochastic mean response to the deterministic logistic map. For the financial application, we use rolling 10 year windows of U.S. broker-dealer customer receivables relative to equity capital. All eligible estimated growth coefficients based on the data lie closer to the lower equilibrium branch, while discrepancies reveal departures from this benchmark around periods of financial disruption. The results connect moment equilibrium of the stochastic model and deterministic transition boundaries with observed financial adjustment, providing a model-based interpretation of these changes without establishing financial chaos.

Keywords: stochastic logistic difference equation; moment equilibrium; lognormal moments; lognormal maximum likelihood; least-squares estimation; financial time series; dynamical transitions

1. Introduction

Discrete logistic models provide a classical setting for examining how proportional expansion and nonlinear constraints interact to produce different patterns of adjustment. Despite their simple form, these models can exhibit convergence to a steady state, periodic oscillations, and chaotic dynamics as the growth parameter changes [1]. Their explicit fixed points and well-understood transition boundaries make them useful benchmarks for investigating how random perturbations and moment variability relate to changes in observed dynamics.

Nonlinear models have a substantial history in economics and finance. Hsieh [2] examines nonlinear financial dynamics and the difficulty of distinguishing deterministic chaos from stochastic variation. Brock et al. [3] show how heterogeneous beliefs can generate complex asset-price dynamics, while Tarasova et al. [4] derive logistic-type maps with memory from an economic growth model incorporating crisis effects. These studies motivate the use of nonlinear feedback to describe economic and financial adjustment. Building on this perspective, we use a simple stochastic logistic model as a local description of customer receivables relative to broker-dealer equity capital, combining state-dependent adjustment with multiplicative random perturbations.

Stochastic models are widely used in mathematical finance to describe the evolution of financial quantities under uncertainty. For example, Shreve [5] develops discrete-time financial models in which random changes determine subsequent asset values. Following this general modeling perspective, we describe financial credit adjustment through a stochastic difference equation. The logistic component represents proportional expansion moderated by a quadratic constraint, while multiplicative noise incorporates random variation in the adjustment process. Lognormal distributions are widely used in financial modeling [6]. This motivates our use of lognormal-form input moments, without requiring a complete lognormal distribution for the financial ratio studied here.

Stochastic difference equations are widely used to describe discrete-time dynamics under random influences across many fields, including biology and finance. Schreiber [7] provides a review of persistence in stochastic population models. Using a distribution-based approach, Wang et al. [8, 9] connect moment-equilibrium conditions with dynamical transitions in stochastic logistic and Ricker equations, while Wang et al. [10] investigate the stability and bifurcation of difference equations arising from stochastic logistic models. Further analyses of logistic models with additive or multiplicative noise show how random variation can alter equilibrium branches and produce saddle-node bifurcations [11, 12].

In this paper, we extend the distribution-based approach of Wang et al. [8, 9] from gamma-distributed population models to a stochastic logistic model with lognormal-form input moments, motivated by applications to positive financial quantities. We retain their moment-equilibrium viewpoint: The incoming and outgoing states have equal means and variances. Assuming the first four input moments have lognormal form, we explicitly obtain two growth branches in terms of input dispersion and multiplicative noise variability. Both real nondegenerate branches remain below the deterministic first period-doubling boundary, while an exact variance correction connects the stochastic mean response to the deterministic model.

In addition, we use quarterly U.S. broker-dealer customer receivables relative to equity capital to estimate the growth coefficient and compare it with the reconstructed equilibrium branches. Within rolling 10 year windows, likelihood and conditional-mean least-squares estimates agree closely under common normalization. All eligible estimates are closer to the lower equilibrium branch than to the upper branch. Their discrepancies from the lower branch describe changes in compatibility with moment equilibrium, including pronounced departures around the 2008 financial crisis and the 2020 pandemic. These observations provide an economic context for interpreting changes in financial adjustment.

The paper is organized as follows: Section 2 introduces the normalized stochastic logistic model and its moment assumptions. Section 3 develops the exact mean correction and deterministic benchmark. Section 4 derives and verifies the explicit moment branches. Section 5 describes the data

and conditional estimation. Section 6 reports the comparisons and economic interpretation. The final section discusses scope and limitations.

2. The stochastic logistic model

We begin with a financial activity variable x_t measured before normalization. In the application, this is customer receivables relative to broker-dealer equity capital. A simple proportional response would give $x_{t+1} = rx_t$, where $r > 0$ is a gross one-period response coefficient. Thus r measures the scale of next-period activity relative to current activity in the absence of constraints on expansion. Existing credit relationships and financing activity motivate this proportional component.

Nonlinear difference equations provide a simple framework for economic adjustment, as illustrated by Stutzer's analysis of discrete-time growth dynamics [13]. Stochastic models are also standard tools for describing financial evolution under uncertainty [5]. Motivated by these approaches, we use a stochastic logistic equation to represent proportional expansion moderated by a quadratic constraint, with multiplicative noise describing random variation in financial adjustment.

Our modeling approximation is that the proportional response is reduced by a fraction that increases linearly with current activity, with coefficient $1/K$, where $K > 0$ is a scale parameter describing the strength of constraints on expansion. The resulting deterministic update is

$$x_{t+1} = rx_t\left(1 - \frac{x_t}{K}\right) = \underbrace{rx_t}_{\text{proportional response}} - \underbrace{\frac{r}{K}x_t^2}_{\text{constraint correction}}. \tag{2.1}$$

The negative quadratic term represents the increasing effect of funding limits, margin requirements, and risk controls as activity rises. Here K is the scale at which this quadratic response vanishes. When $r > 1$, the positive deterministic fixed point is $x^* = K(1 - 1/r)$. Both r and K are treated as constant within an estimation window, while different windows may have different parameter values.

Assume that X_t and x_t are random variables, and set $X_t = x_t/K$, and apply the same K to both members of a transition pair. Dividing (2.1) by K yields

$$X_{t+1} = rX_t(1 - X_t).$$

We allow random perturbations in the realized adjustment by multiplying the response by a positive noise term:

$$X_{t+1} = rX_t(1 - X_t)\xi_{t+1}, \qquad r > 0. \tag{2.2}$$

Here X_{t+1} and X_t are random variables. The noise is independent of X_t and satisfies

$$\mathbb{E}[\xi_{t+1}] = 1, \qquad v = \mathbb{E}[\xi_{t+1}^2] \geq 1, \qquad \mathrm{Var}(\xi_{t+1}) = v - 1. \tag{2.3}$$

We consider a single transition of the stochastic logistic model, with multiplicative noise representing random variation proportional to the model response. The mean-one assumption ensures that r governs the conditional mean response. The moment analysis uses the first four input moments and equality of the incoming and outgoing mean and variance, without requiring a particular noise distribution. In the financial analysis and related simulations, we treat r and the noise parameters as constant within each window and pool consecutive input–output pairs to estimate them. The pooled input observations

approximate a common local moment state. Observed inputs are normalized to ensure positive model responses, as described in Section 5. Future work could extend this framework to additive noise and examine its effects on moment equilibrium and bifurcation behavior, following the direction studied by Yang et al. [11].

3. Small-variance connection to the deterministic model

We first identify the deterministic transition benchmark and then connect it to the stochastic mean. The connection is particularly simple for a quadratic map: The variance correction is exact.

3.1. Deterministic fixed point and first transition boundary

Consider the deterministic logistic equation $x_{t+1} = f_r(x_t)$, where $f_r(x) = rx(1 - x)$. For $r > 1$, its positive fixed point is $x^* = 1 - 1/r$. The derivative at this fixed point is

$$f_r'(x^*) = r(1 - 2x^*) = 2 - r.$$

It governs the local evolution of a small perturbation. The fixed point is locally asymptotically stable when $|2 - r| < 1$, equivalently $1 < r < 3$. At $r = 3$, the derivative reaches -1, marking the first period-doubling boundary. For $r > 3$, the fixed point is unstable, and further increases in r can produce periodic and chaotic dynamics [1]. For $0 < r \leq 1$, there is no positive fixed point.

3.2. Exact variance correction and the small-variance limit

Theorem 1 (Exact mean connection)**.** *Suppose* (2.2) *holds with an independent mean-one noise, and X_t has finite second moment. Then*

$$\mathbb{E}[X_{t+1}] = r\mathbb{E}[X_t](1 - \mathbb{E}[X_t]) - r\,\mathrm{Var}(X_t). \tag{3.1}$$

For fixed r, the difference between the stochastic mean update and the deterministic update tends to zero as $\mathrm{Var}(X_t) \to 0$.

Proof. The independence of ξ_{t+1} and (2.3) give

$$\mathbb{E}[X_{t+1}] = r\{\mathbb{E}[X_t] - \mathbb{E}[X_t^2]\}.$$

Since $\mathbb{E}[X_t^2] = \mathbb{E}[X_t]^2 + \mathrm{Var}(X_t)$, substitution yields (3.1). Its difference from $f_r(\mathbb{E}[X_t])$ is exactly $-r\,\mathrm{Var}(X_t)$, proving the limit without a Taylor expansion or a density assumption. □

The proof is almost identical to that in [9]. The stochastic correction is always negative for $r > 0$: input heterogeneity lowers the next mean relative to applying the logistic map to the mean. The exact identity continues to hold at larger variance even when the deterministic approximation is inaccurate.

4. Lognormal moment equilibrium and explicit feedback branches

We assume the first four input moments have lognormal form,

$$\mathbb{E}[X_t^j] = e^{jm + j^2 s/2}, \qquad j = 1, 2, 3, 4, \qquad m \in \mathbb{R}, s > 0. \tag{4.1}$$

In particular, the mean is

$$\mu = \mathbb{E}[X_t] = e^{m+s/2} > 0,$$

and the variance is

$$\mathrm{Var}(X_t) = \mathbb{E}[X_t^2] - \mu^2 = e^{2m+2s} - e^{2m+s} = \mu^2(e^s - 1).$$

A lognormal input satisfies (4.1), but only the four moment identities are required in the following analysis. These identities need not specify a complete input distribution. A lognormal variable with $\log X_t \sim N(m, s)$, where $m \in \mathbb{R}$ and $s > 0$, has density

$$f_{X_t}(x) = \frac{1}{x\sqrt{2\pi s}} \exp\left[-\frac{(\log x - m)^2}{2s}\right], \qquad x > 0,$$

and $f_{X_t}(x) = 0$ for $x \le 0$. Its moments satisfy (see [15, Chapter 14])

$$\mathbb{E}[X_t^j] = \exp\left(jm + \frac{j^2 s}{2}\right), \qquad j = 1, 2, 3, 4.$$

In this paper, however, (4.1) specifies four moments only: It does not assert $\log X_t \sim N(m, s)$.

A moment-equilibrium transition preserves

$$\mathbb{E}[X_{t+1}] = \mathbb{E}[X_t], \qquad \mathrm{Var}(X_{t+1}) = \mathrm{Var}(X_t). \tag{4.2}$$

Equivalently, it preserves the mean and second raw moment. This definition does not impose equality of complete distributions or full stationarity, and it does not require any marginal distribution for X_{t+1}.

In the empirical analysis, the observed inputs are normalized to $X_t \in (0, 1)$ which ensures $X_{t+1} \in (0, \infty)$. If a realization has $X_t \in (1, \infty)$, positive multiplicative noise gives $X_{t+1} \in (-\infty, 0)$. Such outputs are allowed in the theoretical moment calculation. Nevertheless, since our model (2.2) is a one-step iteration, the moment-equilibrium conditions in (4.2) ensure that the mean and variance of X_{t+1} are positive in the theoretical derivation.

4.1. Two growth branches for moment equilibrium

Theorem 2 (Explicit growth coefficients for a one-step transition)**.** *Under* (2.2)*,* (2.3)*,* (4.1)*, and* (4.2)*, solving the combined mean- and variance-equilibrium conditions gives, for $s > 0$, the following explicit growth coefficients in terms of s and v:*

$$r_\pm(s, v) = \frac{e^{3s} - e^s \pm \sqrt{\dfrac{e^{3s} - 2e^s + 1}{v} - e^{2s}(e^s - 1)}}{e^{3s} - 2e^s + 1}. \tag{4.3}$$

For $v > 1$, these solutions are real if and only if

$$1 < v \le v_{\max}(s) := 1 + e^{-s} - e^{-2s}. \tag{4.4}$$

Throughout this range,

$$1 < r_-(s, v) \le r_+(s, v) < 3. \tag{4.5}$$

The roots coincide at $v = v_{\max}(s)$ and are distinct below it.

Proof of Theorem 2. Taking expectations in the stochastic logistic equation and using independence together with $\mathbb{E}[\xi_{t+1}] = 1$, we obtain

$$\mathbb{E}[X_{t+1}] = r\mathbb{E}[X_t(1 - X_t)]\mathbb{E}[\xi_{t+1}] = r(M_1 - M_2),$$

where $M_j := \mathbb{E}[X_t^j] = e^{jm+j^2 s/2}$, $j = 1, 2, 3, 4$. Similarly, squaring the update and using $\mathbb{E}[\xi_{t+1}^2] = v$ gives

$$\begin{aligned}\mathbb{E}[X_{t+1}^2] &= r^2\mathbb{E}[X_t^2(1 - X_t)^2]\mathbb{E}[\xi_{t+1}^2] \\ &= vr^2\mathbb{E}[X_t^2 - 2X_t^3 + X_t^4] \\ &= vr^2(M_2 - 2M_3 + M_4).\end{aligned}$$

Equality of the incoming and outgoing means and variances also implies equality of their second raw moments. Hence the moment-equilibrium conditions become

$$M_1 = r(M_1 - M_2), \qquad M_2 = vr^2(M_2 - 2M_3 + M_4). \tag{4.6}$$

It explains why moments through order four are required even though only mean and variance are being preserved. Since $M_2/M_1 = e^{m+3s/2}$, the first equality yields

$$r = \frac{1}{1 - e^{m+3s/2}}.$$

A finite positive solution requires $e^{m+3s/2} < 1$, and hence $r > 1$.

Divide the second equality by M_2 and use $M_3/M_2 = e^{m+5s/2}$ and $M_4/M_2 = e^{2m+6s}$:

$$1 = vr^2\left(1 - 2e^{m+5s/2} + e^{2m+6s}\right).$$

Since $e^{m+3s/2} = 1 - 1/r$, it follows that

$$e^{m+5s/2} = e^s\left(1 - \frac{1}{r}\right), \quad e^{2m+6s} = e^{3s}\left(1 - \frac{1}{r}\right)^2.$$

The second-moment equation therefore becomes

$$\frac{1}{v} = r^2 - 2e^s r(r - 1) + e^{3s}(r - 1)^2,$$

and

$$(e^{3s} - 2e^s + 1)r^2 - 2(e^{3s} - e^s)r + e^{3s} - \frac{1}{v} = 0. \tag{4.7}$$

The quadratic formula simplifies to (4.3). For real roots, the discriminant of (4.7) must be nonnegative. It is

$$4\left[(e^{3s} - e^s)^2 - (e^{3s} - 2e^s + 1)(e^{3s} - 1/v)\right] = 4\left[\frac{e^{3s} - 2e^s + 1}{v} - e^{2s}(e^s - 1)\right].$$

For $s > 0$,

$$e^{3s} - 2e^s + 1 = (e^s - 1)(e^{2s} + e^s - 1) > 0.$$

Since $v \geq 1$, the nonnegative-discriminant condition can be written

$$v\, e^{2s}(e^s - 1) \leq e^{3s} - 2e^s + 1.$$

Dividing by the positive quantity $e^{2s}(e^s - 1)$ and factoring the numerator gives

$$v \le \frac{e^{3s} - 2e^s + 1}{e^{2s}(e^s - 1)} = \frac{(e^s - 1)(e^{2s} + e^s - 1)}{e^{2s}(e^s - 1)} = 1 + e^{-s} - e^{-2s} =: v_{\max}(s). \tag{4.8}$$

Every step is reversible because the quantities multiplied or divided are positive, establishing necessity and sufficiency. Thus the bound follows exactly from matching the two moments, without choosing a noise distribution.

For fixed $s > 0$, the expression

$$\frac{e^{3s} - 2e^s + 1}{v} - e^{2s}(e^s - 1)$$

decreases strictly with v. Hence the lower root rises and the upper root falls from $v = 1$ until they coincide at $v = v_{\max}(s)$.

Now for $v = 1$, noting $e^{2s} + e^s > 2$ for $s > 0$, the algebraic roots are

$$r_- = \frac{e^{3s} - e^s - (e^s - 1)}{e^{3s} - 2e^s + 1} = 1, \qquad r_+ = \frac{e^{2s} + e^s + 1}{e^{2s} + e^s - 1} = 1 + \frac{2}{e^{2s} + e^s - 1} < 3.$$

This proves (4.5). □

4.2. Connection with complex dynamics and chaos

Our analysis extends the moment-equilibrium framework of Wang et al. [9] by replacing their gamma distribution assumption with four lognormal-form input moments, motivated by financial applications. As shown in Figure 1, this change produces a different explicit parameterization of the two equilibrium branches in terms of input dispersion and multiplicative noise variability, without requiring a complete input distribution. We also compare these branches with transition coefficients estimated from financial observations, using their discrepancy from the lower branch to describe departures from the equilibrium benchmark.

The present four-moment specification gives a parallel conclusion without assuming a full gamma or lognormal input law. Theorem 2 proves $1 < r_- \le r_+ < 3$ whenever the nondegenerate roots are real. This bound follows directly from the moment equations. The lower and upper branches therefore represent two possible feedback strengths compatible with moment equilibrium. Both remain on the pre-flip side of the deterministic benchmark.

The upper endpoint illustrates the direction of the theoretical comparison. At $v = 1$, the nontrivial algebraic endpoint is

$$r_+(s, 1) = \frac{e^{2s} + e^s + 1}{e^{2s} + e^s - 1} < 3, \qquad r_+(s, 1) \longrightarrow 3 \quad \text{as } s \downarrow 0.$$

For fixed s, increasing v lowers the upper branch and raises the lower branch until they meet.

To make the connection precise, the deterministic logistic map has positive fixed point $x^* = 1 - 1/r$ and derivative $2 - r$. Its first loss of fixed-point stability occurs at $r = 3$; beyond that boundary, further parameter changes may generate period doubling and more complex dynamics [1]. Theorem 1 indicates that the same deterministic map is relevant to the stochastic mean when the variance correction is small.

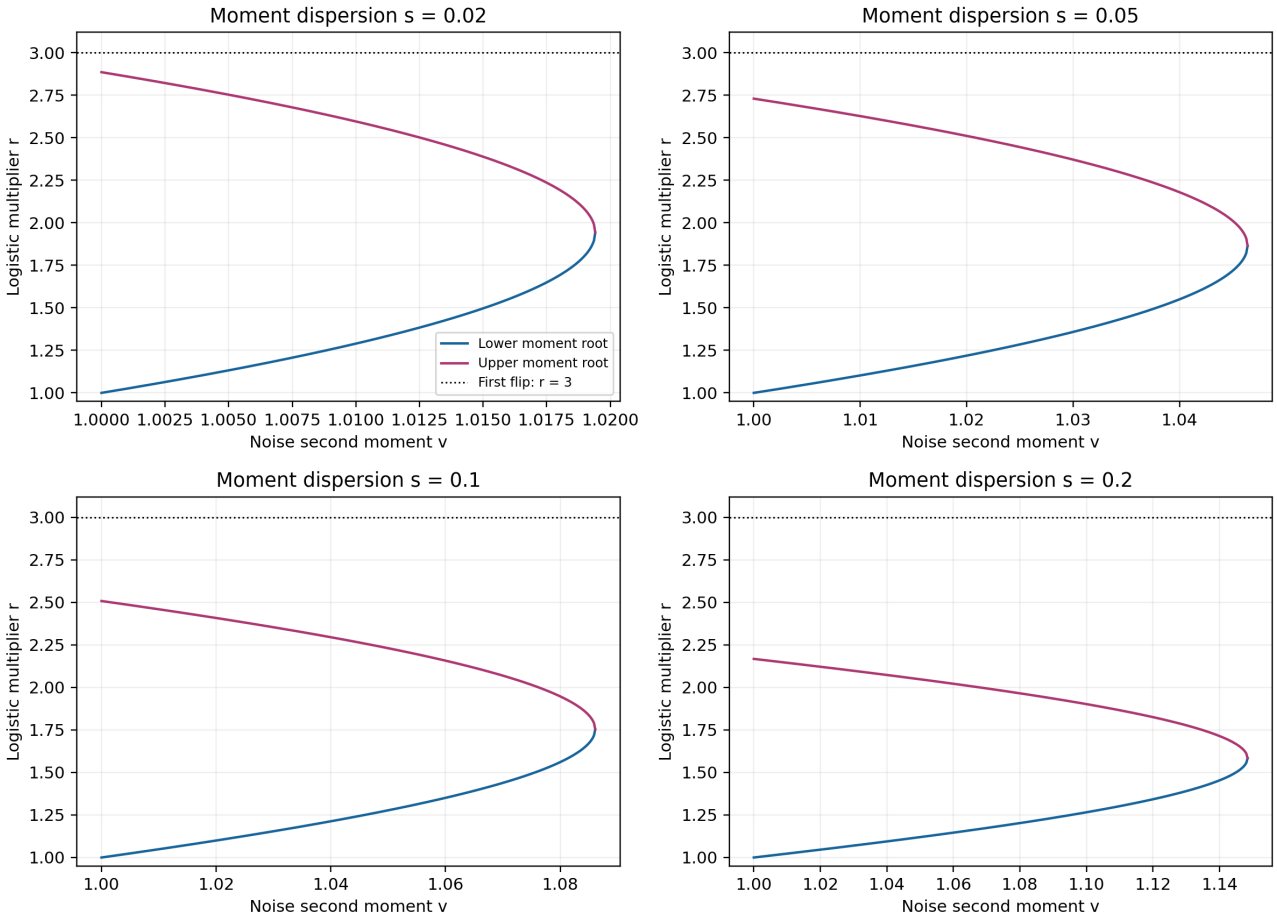


Figure 1. Explicit lower and upper logistic moment growth versus noise second moment, at four prescribed dispersions. The dotted line is the deterministic first-flip boundary $r = 3$. All nondegenerate real roots lie below this boundary.

The upper boundary $r_+(s, 1) < 3$, therefore identifies a possible transition from stable fixed-point behavior to oscillatory dynamics if the growth coefficient increases sufficiently. In the financial application, however, as shown in Figure 2, the estimated coefficients lie around the lower moment-equilibrium branch and remain well below this boundary. Through the small-variance mean connection, these estimates are consistent with an adjustment regime that is distant from the deterministic onset of sustained oscillations and subsequent routes toward chaos. This comparison suggests limited evidence for such a transition in the present data, although it does not quantify the probability of oscillations or chaos in the stochastic model. Our data instead give growth estimates below the first flip. This is consistent with the restricted moment-equilibrium family, not a general claim that financial time series or all stochastic logistic models are nonchaotic.

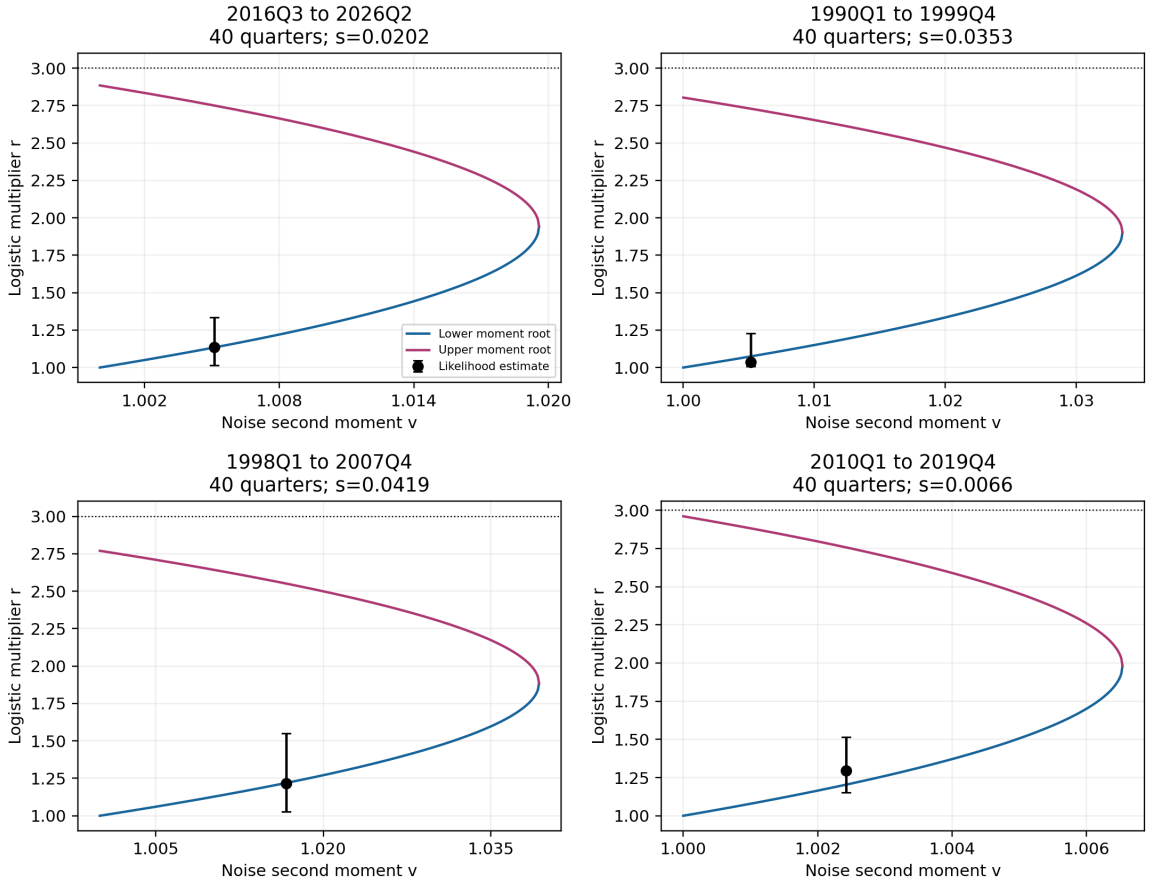


Figure 2. Explicit moment branches and financial likelihood estimates in four calendar-selected windows. Black points are $(\widehat{v}, \widehat{r})$; vertical bars show paired-bootstrap uncertainty in $\widehat{r}$. The dotted horizontal reference is $r = 3$.

5. Financial data, model estimation, and verification

5.1. Data and observation windows

The source series are Federal Reserve Financial Accounts customer receivables and equity capital, distributed through FRED [14] as `BOGZ1FL663067003Q` and `BOGZ1FL665080003Q`. Both are quarterly, end-of-period, not seasonally adjusted, and in millions of dollars; their ratio is dimensionless. The numerator measures customer receivables on securities brokers' and dealers' balance sheets, representing amounts owed by customers; the denominator is the sector's equity capital. Their ratio therefore measures customer credit exposure relative to the intermediaries' own equity capital. For example, a ratio of two means two dollars of customer receivables per dollar of equity capital. A higher ratio indicates more customer credit exposure relative to equity, and a lower ratio indicates less. The retained source tables identify September 11, 2026 as their source update. Early quarterly entries are missing; the continuous analysis sample is 1952:Q1–2026:Q2, with 298 observations and no interpolation. Dates such as 2026-04-01 label quarters.

We use one window length throughout: 40 quarterly observations (10 years), giving 39 consecutive transition pairs per window. With 298 quarterly observations, advancing the window by one quarter gives $298 - 40 + 1 = 259$ windows. The first runs from 1952:Q1 to 1961:Q4 and the last from 2016:Q3 to 2026:Q2. Adjacent windows share 39 observations and 38 transition pairs.

Within each window, we divide the observed financial ratios by a common positive scale K exceeding all input observations, giving normalized input and output values denoted throughout by X_t and X_{t+1}. The same scale is used on both sides of every pair and is calibrated jointly with the transition parameters; it is allowed to differ between windows. Its numerical profiling is an implementation detail retained in the code. A calibration reaching the proportional-growth boundary does not provide a finite normalization and is flagged separately.

The theoretical model considers one transition at a specified time. The observed series supplies only one pair at that time, so we pool 39 pairs with different dates within each window. This approximates a common local transition law and input moment state: r, the noise moments, and the input moments are treated as approximately constant within the window. Such local homogeneity is an empirical modeling approximation. It can fail during abrupt financial changes. The 40-quarter choice keeps the analysis focused on a shorter historical period while providing multiple pairs.

5.2. Financial modeling and two estimation methods

The normalized financial observations are modeled by (2.2). For the empirical estimation, we require

$$X_t \in (0, 1), \tag{5.1}$$

so the logistic factor is positive. The parameter r measures logistic adjustment.

Method 1: lognormal-noise likelihood. We assume independent mean-one lognormal multiplicative noise,

$$\xi_{t+1} = \exp\left(\sqrt{s_\xi}\, \varepsilon_{t+1} - \frac{s_\xi}{2} \right), \qquad \varepsilon_{t+1} \sim N(0, 1),$$

where ε_{t+1} is independent of X_t. The correction $-s_\xi/2$ ensures $\mathbb{E}[\xi_{t+1}] = 1$. Taking logarithms conditional on $X_t = x$ gives

$$\log X_{t+1} \mid X_t = x \sim N\left(\log[rx(1 - x)] - \frac{s_\xi}{2}, s_\xi \right). \tag{5.2}$$

For a fixed normalization, estimation can be simplified by transforming each observed transition pair:

$$z_t := \log\left(\frac{X_{t+1}}{X_t(1 - X_t)} \right) = \log r - \frac{s_\xi}{2} + \sqrt{s_\xi}\, \varepsilon_{t+1}.$$

Thus the transformed observations are normally distributed with mean $\log r - s_\xi/2$ and variance s_ξ. Writing $\bar{z} = N^{-1} \sum_{t=1}^{N} z_t$, the maximum-likelihood estimates are

$$\widehat{s_\xi} = \frac{1}{N} \sum_{t=1}^{N} (z_t - \bar{z})^2, \qquad \widehat{r}_{\mathrm{ML}} = \exp\left(\bar{z} + \frac{\widehat{s_\xi}}{2} \right).$$

Since mean-one lognormal noise satisfies $\mathbb{E}[\xi_{t+1}^2] = e^{s_\xi}$, its estimated second moment is

$$\widehat{v}_{\mathrm{ML}} = e^{\widehat{s}_\xi}.$$

When the normalization scale is also estimated, these formulas are evaluated at each candidate scale, and the scale maximizing the conditional likelihood is selected.

Method 2: conditional-mean least squares. Suppose only that $\mathbb{E}[\xi_{t+1}] = 1$. For a fixed set of normalized pairs, define $F_t = X_t(1 - X_t)$ and minimize $\sum_{t=1}^{N}(X_{t+1} - rF_t)^2$. This gives

$$\widehat{r}_{\mathrm{LS}} = \frac{\sum_{t=1}^{N} F_t X_{t+1}}{\sum_{t=1}^{N} F_t^2}. \tag{5.3}$$

This estimates the conditional mean parameter without specifying a full noise distribution.

For comparing with the moment roots, use multiplicative residuals $\widehat{\xi}_{t+1} = X_{t+1}/(\widehat{r}_{\mathrm{LS}}F_t)$ and

$$\widehat{v}_{\mathrm{LS}} = 1 + \frac{1}{N}\sum_{t=1}^{N}(\widehat{\xi}_{t+1} - 1)^2. \tag{5.4}$$

The identity $v = 1 + \mathbb{E}[(\xi_{t+1} - 1)^2]$ follows from the mean-one assumption. This estimator respects $v \geq 1$.

Table 1 compares the two estimates on the same normalized pairs in four selected windows. The difference is $\widehat{r}_{\mathrm{LS}} - \widehat{r}_{\mathrm{ML}}$. Its 95% intervals use 500 circular block-bootstrap samples with block length four, holding each window's likelihood-calibrated normalization fixed; all four intervals contain zero. Of the 259 rolling windows, 242 yield a finite estimated normalization scale; the remaining 17 approach the proportional-growth limit. We compare the two estimators on the same normalized pairs in these 242 windows. Across all 242 finite-scale windows, the median absolute difference is 0.000371, and the maximum is 0.019476. The estimates therefore agree closely under a common normalization.

Table 1. Two estimators on identical normalized pairs. Intervals refer to the paired least squares -minus-likelihood difference, conditional on the window's fixed normalization.

Period	$\widehat{r}_{\mathrm{ML}}$	$\widehat{r}_{\mathrm{LS}}$	Difference	95% interval
2016:Q3–2026:Q2	1.134837	1.134909	0.000072	[−0.00677, 0.00591]
1990:Q1–1999:Q4	1.035304	1.035530	0.000226	[−0.00962, 0.00899]
1998:Q1–2007:Q4	1.216267	1.215935	−0.000332	[−0.01869, 0.01656]
2010:Q1–2019:Q4	1.297028	1.297037	0.000008	[−0.00171, 0.00183]

6. Empirical results and financial departures from equilibrium

6.1. Empirical estimates and the moment-equilibrium branches

Across the 259 windows, the estimated growth ranges from 0.9574 to 1.4819. Of these profiles, 242 admit finite normalization, and 17 reach the proportional-growth boundary. Among the finite-scale

fits, 11 have $r \leq 1$, which is incompatible with positive mean equilibrium in the logistic model. The 231 finite-scale fits with $r > 1$ are all closer to the lower moment root than the upper root.

Table 2. Calendar-selected windows: logistic likelihood fits and explicit moment roots for the normalized observations.

Period	n	$\widehat{s}$	$\widehat{v}$	$\widehat{r}$	r_-	r_+
2016:Q3–2026:Q2	40	0.02018	1.005107	1.134837	1.134172	2.749828
1990:Q1–1999:Q4	40	0.03535	1.005138	1.035304	1.074079	2.728967
1998:Q1–2007:Q4	40	0.04187	1.016673	1.216267	1.218821	2.550920
2010:Q1–2019:Q4	40	0.00660	1.002422	1.297028	1.203657	2.757310

The four detailed fits all admit finite normalization and have $r > 1$. Input and output values use a common scale within each window, while the scale may differ between windows. In the latest window, $\widehat{r} = 1.134837$ and $r_- = 1.134172$ are particularly close. Its paired-bootstrap 95% discrepancy interval is $[-0.1944, 0.1457]$. It contains zero but is broad.

Figure 2 and Table 2 compare two different quantities. The estimate $\widehat{r}$ is obtained from the observed consecutive pairs using the conditional likelihood in Section 5.2. Theorem 2 gives $r_-(s, v)$ and $r_+(s, v)$ by solving those two equilibrium conditions under the four prescribed input moments. We insert the window's estimated input dispersion $\widehat{s}$ and noise second moment $\widehat{v}$ into that theorem. The resulting roots are the growth coefficients compatible with the moment-equilibrium specification.

In each panel of Figure 2, the curves show how these moment-equilibrium candidates vary with v while holding the window's $\widehat{s}$ fixed. The black point uses the actual fitted pair $(\widehat{v}, \widehat{r})$, and its vertical interval describes bootstrap uncertainty in the transition estimate. The visual comparison is therefore made at the observed $\widehat{v}$. Table 2 gives the corresponding numerical values. For example, the latest window gives $\widehat{r} = 1.134837$ and $r_- = 1.134172$, whereas $r_+ = 2.749828$ is much farther away. The 1998:Q1–2007:Q4 window similarly gives $\widehat{r} = 1.216267$ and $r_- = 1.218821$. The 2010:Q1–2019:Q4 values, $\widehat{r} = 1.297028$ and $r_- = 1.203657$, show that lower-branch proximity need not mean exact agreement.

These comparisons are consistent with the lower moment-equilibrium branch for the selected windows and for all 231 eligible rolling fits. Theorem 2 places both real nondegenerate branches below $r = 3$; the observed estimates also remain below this first-flip boundary without imposing that constraint during fitting. Thus the data comparison supports a pre-flip adjustment regime and allows departures from moment equilibrium, rather than identifying chaos in the financial series.

6.2. Noise admissibility and the bound $v_{\max}(s)$

The discriminant calculation in the proof of Theorem 2, specifically (4.8), gives $v_{\max}(s) = 1 + e^{-s} - e^{-2s}$. We now discuss its interpretation and compare it with the financial estimates.

Because $\mathrm{Var}(\xi) = v - 1$, the admissibility condition is

$$\mathrm{Var}(\xi) \leq e^{-s}(1 - e^{-s}). \tag{6.1}$$

The right-hand side increases for $0 < s < \log 2$, has maximum $1/4$ at $s = \log 2$, and decreases thereafter. This follows by setting $z = e^{-s} \in (0, 1)$ and maximizing $z(1 - z)$. Consequently, $v \leq 5/4$ is necessary for any member of this moment-equilibrium family.

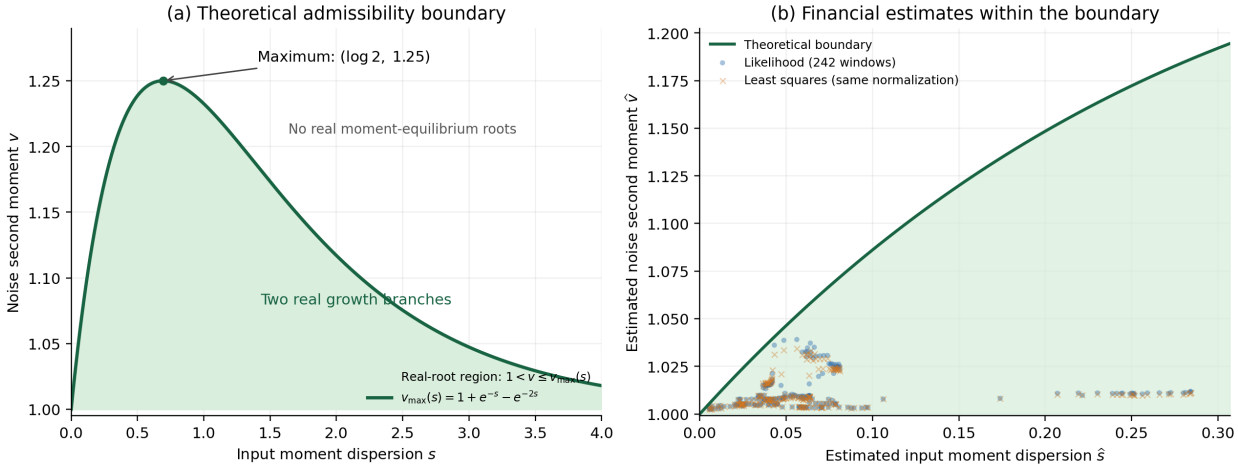


Figure 3. The noise admissibility boundary and financial estimates. (a) The curve $v_{\max}(s) = 1 + e^{-s} - e^{-2s}$ bounds the shaded real-root region. Its maximum is $5/4$ at $s = \log 2$. (b) Estimates $(\widehat{s}, \widehat{v})$ for all 242 finite-scale windows under likelihood (blue circles) and conditional-mean least squares (orange crosses), using the same normalization. Windows each contain 40 quarterly observations and overlap. All estimates lie below the boundary.

At $v = v_{\max}(s)$, the two algebraic roots merge because the discriminant vanishes. For $v > v_{\max}(s)$, there is no real growth coefficient satisfying both equilibrium equations with the prescribed moment dispersion.

Figure 3 displays the complete admissibility curve and an enlarged view over the observed dispersion range. The boundary peaks at $s = \log 2$, where $v_{\max} = 1.25$; points strictly below it and above $v = 1$ give two distinct real moment-equilibrium branches. On the boundary, the branches coincide. The estimates from both methods lie below the curve, so the real-root condition is satisfied in every finite-scale window.

6.3. Financial-crisis and pandemic interpretations

The model analysis provides a useful indication of changes in financial adjustment through departures from the moment-equilibrium benchmark. We illustrate this interpretation during the recession periods associated with the 2008 financial crisis and the 2020 COVID-19 pandemic. The shaded bands in both panels of Figure 4 mark the recession periods associated with the 2008 financial crisis and the 2020 COVID-19 pandemic. They provide context for interpreting changes in the estimated coefficient $\widehat{r}$ and the discrepancy δ_- defined below.

For a rolling window W of 40 quarterly observations, define

$$\delta_-(W) = \widehat{r}(W) - r_-\big(\widehat{s}(W), \widehat{v}(W)\big)\,. \tag{6.2}$$

The first term is the transition coefficient estimated from the 39 observed consecutive pairs in W. The second term is calculated from Theorem 2, using the same window's input moment dispersion and noise second moment. Thus δ_- compares an empirical transition estimate with a model-implied equilibrium candidate.

The lower branch is the relevant comparison because all eligible rolling estimates are closer to it

than to the upper branch. A value near zero means that fitted adjustment is close to the lower candidate implied by the window's dispersion and noise. A positive value means the fitted coefficient exceeds that candidate; a negative value means it is smaller. Holding the normalized input x fixed, the difference between the two mean response curves is

$$\widehat{r}x(1-x) - r_{-}(\widehat{s},\widehat{v})x(1-x) = \delta_{-}x(1-x).$$

For $0 < x < 1$, its sign agrees with that of δ_{-}. This gives a direct interpretation in the stochastic logistic model: the fitted conditional response is above or below the lower-equilibrium benchmark at the same input and normalization.

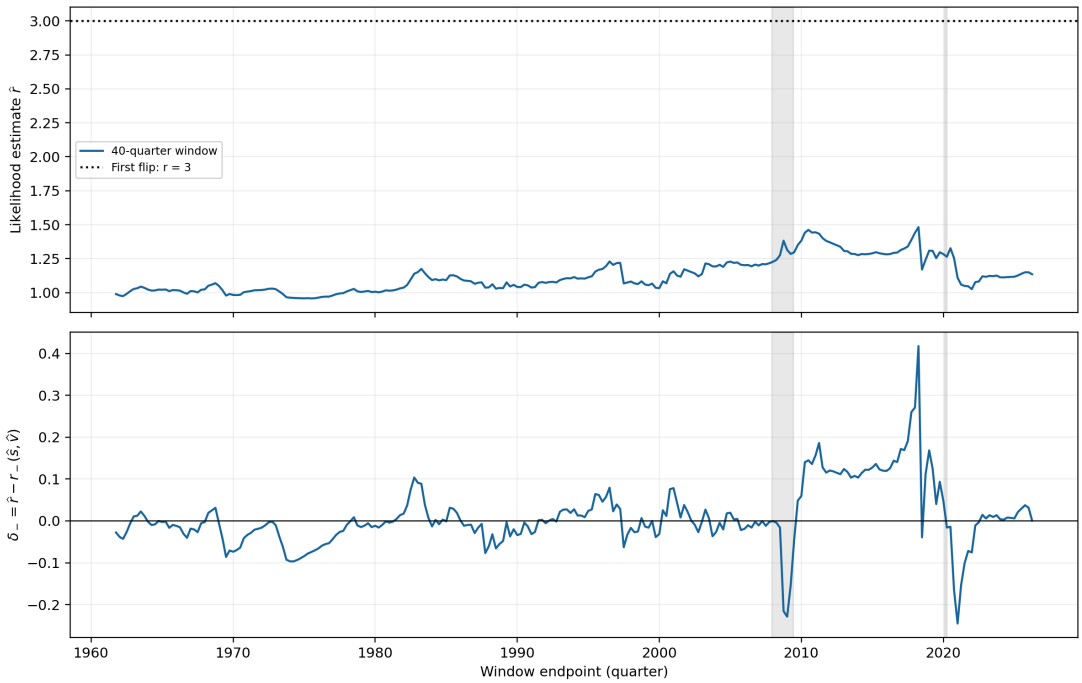


Figure 4. Conditional logistic likelihood estimates of r (top), and differences from the lower moment-equilibrium branch (bottom). All rolling estimates, including flagged boundary and subunit estimates, are shown. Gray bands mark the recession periods associated with the 2008 financial crisis and the 2020 COVID-19 pandemic.

Figure 4 shows the fitted growth coefficient in its top panel and the discrepancy δ_{-} defined in (6.2) in its bottom panel. Around the 2008 recession and financial crisis, the discrepancy displays a marked negative departure from zero. This indicates that the fitted coefficient falls below the lower moment-equilibrium benchmark, even as the coefficient itself increases. A plausible interpretation is that abrupt financial adjustment during the crisis is less compatible with moment equilibrium pooled over the preceding decade. This association provides economic context for the discrepancy without establishing a causal relationship.

Figure 4 shows a decline in the estimated growth coefficient around the 2020 COVID-19 disruption, accompanied by a marked negative departure of δ_{-} from zero. The discrepancy subsequently moves back toward zero, indicating closer agreement with the lower moment-equilibrium benchmark. These changes smay uggest altered financial adjustment during the pandemic.

Taken together, the 2008 and 2020 examples illustrate departures from the lower moment-equilibrium benchmark. A negative δ_- places the fitted response below that benchmark and may be economically informative during periods of changing financial conditions.

7. Discussion and economic implications

This paper develops a moment-equilibrium approach to studying a stochastic logistic model and applies it to financial data. Preserving the input mean and variance yields two explicit growth branches and an exact restriction linking input dispersion with noise variability. Both branches remain below the deterministic first period-doubling boundary. An exact variance correction also connects the stochastic mean response with the deterministic model. Using rolling 10 year windows of the customer-receivables-to-equity ratio, we find close agreement between likelihood and least-squares estimates under common normalization. Eligible estimates consistently lie closer to the lower equilibrium branch. Departures from this benchmark show changes around the financial-crisis and pandemic periods, providing a model-based description of financial adjustment rather than evidence of chaos.

The stochastic logistic model permits an explicit characterization of moment equilibrium. The model yields two growth branches satisfying the combined mean- and variance-equilibrium conditions. Both real nondegenerate branches remain below the deterministic first period-doubling boundary. These results require only four lognormal-form input moments, without specifying the full input or output distribution. In the financial application, normalization places observed inputs within the range of positive logistic responses.

The financial application illustrates how departures from moment equilibrium can describe changes in credit adjustment relative to broker-dealer equity. Using rolling 10 year windows, the estimated growth coefficients lie around the lower equilibrium branch, with all eligible estimates closer to this branch than to the upper branch. Larger discrepancies appear around the 2008 financial crisis and the 2020 pandemic. These departures may reflect changes in financing conditions, input dispersion, or noise variability. The comparison therefore may provide a model-based perspective on financial adjustment. Interpretation must also account for overlapping windows and the influence of earlier observations within each window.

Several limitations should be considered when interpreting these results. The financial analysis pools observations from different dates within each 10 year window, assuming approximately constant transition parameters and input moments; this approximation may fail during rapid changes in financial conditions. Adjacent windows overlap substantially, so their estimates are not independent. The logistic response and four lognormal-form moments are modeling assumptions, and agreement with the lower equilibrium branch does not establish their validity or exact moment preservation. Estimates also depend on normalization and, for likelihood estimation, the chosen noise distribution. The application uses a single financial ratio whose movements can reflect changes in either receivables or equity capital; its historical comparability is further limited by changes in reporting coverage.

Future work could extend the present framework to more general nonlinear models of financial adjustment, allowing for alternative growth responses, delayed feedback, and changing financing constraints. Bifurcation analysis could then examine how input dispersion and noise variance affect

the growth coefficients required to preserve the mean and variance in models with more general nonlinear response terms. Connecting these mathematical transitions with observable changes in financing conditions would further strengthen the economic interpretation of the framework.

Further empirical work could apply the framework to additional financial datasets, including other measures of credit, intermediary leverage, and financing activity. Comparisons across institutions, countries, and historical periods would help assess whether proximity to the lower equilibrium branch and larger discrepancies during financial disruptions persist beyond the present series. Examining alternative window lengths and evaluating performance on subsequent observations would also help establish the robustness and potential predictive value of the approach.

Use of AI tools declaration

The authors declare they have not used Artificial Intelligence (AI) tools in the creation of this article.

Conflict of interest

The authors declare that they have no conflict of interest.

References

1. May RM, (1976) Simple mathematical models with very complicated dynamics. *Nature* 261: 459–467. https://doi.org/10.1038/261459a0
2. Hsieh DA, (1991) Chaos and nonlinear dynamics: Application to financial markets. *J Finance* 46: 1839–1877. https://doi.org/10.1111/j.1540-6261.1991.tb04646.x
3. Brock WA, Hommes CH, (1998) Heterogeneous beliefs and routes to chaos in a simple asset pricing model. *J Econ Dyn Control* 22: 1235–1274. https://doi.org/10.1016/S0165-1889(98)00011-6
4. Tarasova VV, Tarasov VE, (2017) Logistic map with memory from economic model. *Chaos Solitons Fractals* 95: 84–91. https://doi.org/10.1016/j.chaos.2016.12.012
5. Shreve SE, (2004) *Stochastic Calculus for Finance I: The Binomial Asset Pricing Model*, Springer, New York. https://doi.org/10.1007/978-0-387-22527-2
6. Shreve SE, (2004) *Stochastic Calculus for Finance II: Continuous-Time Models*, Springer, New York.
7. Schreiber SJ, (2012) Persistence for stochastic difference equations: A mini-review. *J Differ Equations Appl* 18: 1381–1403. https://doi.org/10.1080/10236198.2011.628662
8. Wang H, (2025) Equilibrium analysis of discrete stochastic population models with gamma distribution. *Math Biosci* 381: 109398. https://doi.org/10.1016/j.mbs.2025.109398
9. Wang H, Wang Y, (2025) Detecting transitions from steady states to chaos with gamma distribution. *Int J Bifurcation Chaos* 35: 2550163. https://doi.org/10.1142/S0218127425501639
10. Wang H, Wang E, (2026) Stability and bifurcation of difference equations from stochastic logistic models. *Math Biosci Eng* 23: 449–473. https://doi.org/10.3934/mbe.2026018

11. Yang Y, Han X, (2027) Equilibrium and bifurcation analysis of a stochastic logistic difference equation with additive noise. *Discrete Contin Dyn Syst S*, 33: 116–138. https://doi.org/10.3934/dcdss.2026151
12. Yang Y, Han X, (2027) Gamma moment-closure and noise-induced saddle-node bifurcation in a stochastic logistic difference equation. *Discrete Contin Dyn Syst S* 33: 420–452. https://doi.org/10.3934/dcdss.2026173
13. Stutzer MJ, (1980) Chaotic dynamics and bifurcation in a macro model. *J Econ Dyn Control* 2: 353–376. https://doi.org/10.1016/0165-1889(80)90070-6
14. Federal Reserve Bank of St. Louis, *Numerical Tables for BOGZ1FL663067003Q and BOGZ1FL665080003Q*. Available from: https://fred.stlouisfed.org/data/BOGZ1FL663067003Q; https://fred.stlouisfed.org/data/BOGZ1FL665080003Q
15. Johnson NL, Kotz S, Balakrishnan N, (1994) *Continuous Univariate Distributions*, Wiley, New York.



AIMS Press

© 2026 the Author(s), licensee AIMS Press. This is an open access article distributed under the terms of the Creative Commons Attribution License (https://creativecommons.org/licenses/by/4.0)